Reentrant Localization Transition in a Quasiperiodic Chain

Shilpi Roy,[1] Tapan Mishra,[1] B. Tanatar,[2] and Saurabh Basu[1]
[1]Department of Physics, Indian Institute of Technology Guwahati-Guwahati, 781039 Assam, India
[2]Department of Physics, Bilkent University, TR-06800 Bilkent, Ankara, Turkey

(Received 9 August 2020; accepted 1 February 2021; published 9 March 2021)

Systems with quasiperiodic disorder are known to exhibit a localization transition in low dimensions. After a critical strength of disorder, all the states of the system become localized, thereby ceasing the particle motion in the system. However, in our analysis, we show that in a one-dimensional dimerized lattice with staggered quasiperiodic disorder, after the localization transition, some of the localized eigenstates become extended for a range of intermediate disorder strengths. Eventually, the system undergoes a second localization transition at a higher disorder strength, leading to all states being localized. We also show that the two localization transitions are associated with the mobility regions hosting the single-particle mobility edges. We establish this reentrant localization transition by analyzing the eigenspectra, participation ratios, and the density of states of the system.

DOI: 10.1103/PhysRevLett.126.106803

Introduction.—The phenomenon of localization of quantum particles which is directly related to the transport properties has been a topic of paramount interest in recent years [1]. Originally proposed in the context of condensed matter systems, this phenomenon deals with the localization of the single-particle wave function in the presence of uncorrelated (random) disorder known as the Anderson localization (AL) [2]. Anderson localization predicts the metal-insulator transition as a result of quantum interference of a scattered wave function in the presence of impurities in the system. This interesting phenomenon has been studied in disparate systems such as photonics lattices and elastic media as well as in optical lattices [3–10].

While the metal-insulator transition associated with the AL is limited to higher-dimensional systems, similar physics can be obtained in one dimension by replacing the uncorrelated (random) disorder by a quasiperiodic potential. The simplest example of such quasiperiodic systems which are neither periodic nor completely disordered is the self-dual Aubry-André (AA) model [11], which exhibits the localization transition at a critical quasiperiodic potential strength before (after) which all the states of the system are extended (localized). However, in certain generalized AA model and other quasiperiodic systems [12–17], the transitions to the localized phases are often associated with a critical region where both extended and localized states coexist. The key feature of this critical region is the existence of the single-particle mobility edge (SPME) which corresponds to a critical energy separating the extended and the localized states of the system [1,18]. Because of the recent progress in the field of quantum gases in optical lattices, the localization transition and the possible existence of the SPME in quasiperiodic systems have gained considerable interest [19,20], leading to their recent experimental observations [21–23].

So far, it has been well established that, after the system undergoes a localization transition, all the states remain localized forever with increasing disorder strength. In this work, we show that this is indeed not always true. In a one-dimensional dimerized lattice with staggered quasiperiodic disorder, the competition between dimerization and quasiperiodic disorder leads to a reentrant localization transition. This means some of the already localized states become extended again for a range of quasiperiodic potential. A further increase in the disorder strength leads to the second localization transition where all the states become localized again. This reentrant localization transition is also associated with separate critical regions hosting the SPMEs in the spectrum.

Model and approach.—We consider a one-dimensional dimerized lattice with on-site quasiperiodic disorder which is given by the Hamiltonian:

$$H = -t_1 \sum_{i=1}^{N} (c_{i,B}^{\dagger} c_{i,A} + \text{H.c.}) - t_2 \sum_{i=1}^{N-1} (c_{i+1,A}^{\dagger} c_{i,B} + \text{H.c.}) + \sum_{i=1}^{N} \lambda_A n_{i,A} \cos[2\pi\beta(2i-1)] + \sum_{i=1}^{N} \lambda_B n_{i,B} \cos[2\pi\beta(2i)]. \quad (1)$$

This is a chain of N unit cells consisting of two sublattice sites A and B. i represents the unit cell index, and $L = 2N$ is the length of the chain. $c_{i,A}^{\dagger}(c_{i,A})$ and $c_{i,B}^{\dagger}(c_{i,B})$ are the creation (annihilation) operators corresponding to sites in the A and B sublattices which we denote by (i, A) and (i, B), and the site number operators are denoted as $n_{i,A}$ and $n_{i,B}$.

The intra- and intercell hopping strengths are represented by t_1 and t_2, respectively, and H.c. stands for the Hermitian conjugate. The strength of the on-site potential at the sublattice site $A(B)$ is represented by λ_A (λ_B), and β determines the period of quasiperiodic potential. The staggered disorder is introduced by assuming $\lambda_A = -\lambda_B = \lambda$ in Eq. (1). The model Eq. (1) in the limit of vanishing disorder, i.e., $\lambda = 0$, is the paradigmatic Su-Schrieffer-Heeger model [24], which exhibits a trivial (when $t_1 > t_2$) to topological (when $t_1 < t_2$) phase transition through a gap closing point at $t_1 = t_2$. This phase transition is protected by the chiral symmetry of the system. Note that in the presence of finite on-site disorder this symmetry is explicitly broken.

We choose $\beta = (\sqrt{5}-1)/2$, a Diophantine number [25] in our work, and fix the intracell hopping $t_1 = 1$ as the energy scale. For convenience, we define a quantity $\delta = t_2/t_1$ which controls the hopping dimerization in Eq. (1). The system size considered in our simulations is up to $L = 13530$, that is, $N = 6765$ unit cells. We explore the effect of staggered disorder in both the limits of dimerization in Eq. (1) such as $\delta < 1$ and $\delta > 1$. To analyze the physics of the model shown in Eq. (1), we rely on the inverse participation ratio (IPR) and the normalized participation ratio (NPR) [20,26], which are the two most significant diagnostic tools to characterize the localization transition. For the nth eigenstate ϕ_n^i, the IPR and the NPR are defined, respectively, as

$$\mathrm{IPR}_n = \sum_{i=1}^{L} |\phi_n^i|^4, \qquad \mathrm{NPR}_n = \left(L \sum_{i=1}^{L} |\phi_n^i|^4 \right)^{-1}. \quad (2)$$

The extended (localized) phases are characterized by $\mathrm{IPR} = 0 (\neq 0)$ and $\mathrm{NPR} \neq 0 (= 0)$ in the large L limit. Before proceeding with the staggered λ case, we first highlight the physics associated with the case of uniform λ for comparison.

Uniform disorder ($\lambda_A = \lambda_B = \lambda$).—In the limit of $\delta = 1$, Eq. (1) corresponds to the pure AA model which exhibits a localization transition without any SPME. However, moving away from this limit, we show that the localization transition occurs through a critical regime hosting the SPME for both $\delta < 1$ and $\delta > 1$. To identify the localization transitions, we plot the $\langle \mathrm{IPR} \rangle$ and the $\langle \mathrm{NPR} \rangle$ as a function of λ for the two exemplary points, namely, $\delta = 0.5$ and $\delta = 3$ in Figs. 1(a) and 1(b), respectively. Here, $\langle \mathrm{IPR} \rangle$ and $\langle \mathrm{NPR} \rangle$ denote the averages of the IPR and NPR, respectively, computed by considering all the eigenstates for a particular value of λ. It can be seen that, contrary to the simple AA model ($\delta = 1$), the plots for the $\langle \mathrm{IPR} \rangle$ and the $\langle \mathrm{NPR} \rangle$ do not sharply cross each other at the duality point $\lambda = 2$ [27] for both values of δ. Rather, they cross each other at very different values of λ and also exhibit a coexisting region where both the $\langle \mathrm{IPR} \rangle$ and the $\langle \mathrm{NPR} \rangle$ are finite (shaded regions). This signifies the presence of both the localized and the extended states for a range of λ ($0.7 < \lambda < 1.4$ when $\delta = 0.5$ and $1.6 < \lambda < 3.4$ when $\delta = 3$) which are the critical phases exhibiting the SPMEs. Clearly, after the localization transition, all the states remain localized as a function of λ.

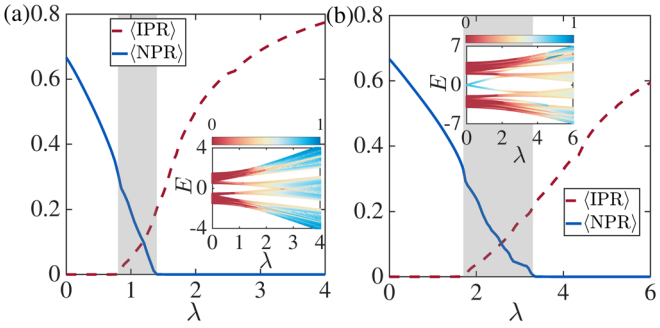

FIG. 1. The $\langle \mathrm{IPR} \rangle$ (red dashed curve) and $\langle \mathrm{NPR} \rangle$ (blue solid curve) are plotted as a function of λ for (a) $\delta = 0.5$ and (b) $\delta = 3$ for a system of size $L = 13530$. The shaded regions indicate the critical or the intermediate regimes. The color maps in the insets show the plots of IPR associated to all eigenmodes E with respect to λ for values of δ of the main figure.

The localization transition and the existence of the SPME can be easily inferred from the energy spectrum and the associated IPR of the individual states. We plot the IPR associated to the energy spectra E corresponding to the Hamiltonian in Eq. (1) for $\delta = 0.5$ and 3 in the insets in Figs. 1(a) and 1(b), respectively. Here, the eigenenergies are color coded with the corresponding IPRs. Because of the dimerized nature of the model [Eq. (1)], we get two distinct energy bands at $\lambda = 0$, and in this limit the energy levels are completely extended for both the trivial [Fig. 1(a)] and the topological [Fig. 1(b)] cases. As the value of λ increases, the gaps between the bands in both the dimerized limits tend to vanish beyond a critical λ. Clearly, in both cases, the fully extended (red) and the localized regions (blue) are separated by a critical phase where both extended and localized states coexist for a range of values of λ which host a SPME. Quite expectedly, the appearance of the localized states at $\lambda = 0$ in the inset in Fig. 1(b) is the topological edge modes present in the middle of the gap. We shall discuss the fate of these edge modes later. Note that other minibands with some states in the gaps between them appear in the energy spectrum due to the quasiperiodic disorder which are irrelevant for the present analysis.

Staggered disorder ($\lambda_A = -\lambda_B = \lambda$).—In this section, we discuss the role of staggered disorder on the localization transition. In this case also, one expects a qualitatively similar localization transition as in the uniform disorder case with some quantitative difference. This is confirmed in our analysis, which shows the extended to localization transition through a critical phase where both $\langle \mathrm{IPR} \rangle$ and $\langle \mathrm{NPR} \rangle$ are finite for a range of values of δ. As is well known and already mentioned before, in quasiperiodic lattices exhibiting localization hosting the SPME, for the values of

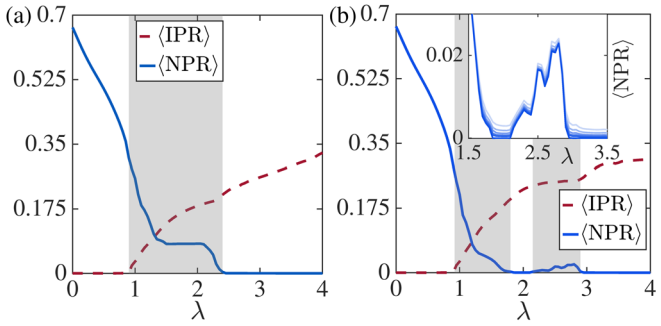

FIG. 2. (a) and (b) show the $\langle \mathrm{IPR} \rangle$ and the $\langle \mathrm{NPR} \rangle$ for $\delta = 1.5$ and 2.2, respectively, for the case of staggered disorder and $L = 13530$. The shaded regions represent the critical phases. The inset shows the $\langle \mathrm{NPR} \rangle$ for $L = 1974$, 3194, 5168, 8362, 13530, and ∞ (light to deep blue).

λ prior to (beyond) the critical phase, all the states of the system are extended (localized).

Once the system is in the localized phase, it remains localized as a function of the strength of the quasiperiodic potential λ. As a result, one gets $\langle \mathrm{IPR} \rangle \neq 0$ and $\langle \mathrm{NPR} \rangle = 0$ for all values of λ after the critical regime. However, surprisingly in the presence of the staggered disorder, we find that, for some intermediate values of δ, the system undergoes two localization transitions through two critical phases as a function of λ. This reentrant localization behavior can be very well discerned by together analyzing the $\langle \mathrm{IPR} \rangle$ and $\langle \mathrm{NPR} \rangle$. In Figs. 2(a) and 2(b), we show the $\langle \mathrm{IPR} \rangle$ and $\langle \mathrm{NPR} \rangle$ corresponding to two different values of dimerization such as $\delta = 1.5$ and 2.2, respectively, for $L = 13530$. Clearly, for $\delta = 1.5$ [Fig. 2(a)], there is a transition to the localized phase through a critical region for the range of λ between $0.9 < \lambda < 2.5$. After the localization transition, i.e., for $\lambda > 2.5$, all the states are localized. On the other hand, for $\delta = 2.2$ [Fig. 2(b)], there exist two critical regions in the range $0.9 < \lambda < 1.8$ and $2.1 < \lambda < 2.9$ where both the $\langle \mathrm{IPR} \rangle$ and $\langle \mathrm{NPR} \rangle$ are finite. In the region between the two critical phases and again beyond the second critical phase, the system is fully localized. This indicates that the system also hosts two SPMEs as a function of λ. Note that the extent of the second critical region occurs for a small range of λ. In order to rule out any finite size effects, we perform finite size extrapolation of the $\langle \mathrm{IPR} \rangle$ [28] and $\langle \mathrm{NPR} \rangle$ considering data for different system sizes such as $L = 1974$, 3194, 5168, 8362, and 13530. The inset in Fig. 2(b) shows the $\langle \mathrm{NPR} \rangle$ data for various system sizes including the one at $L \to \infty$ for $\delta = 2.2$. This clearly indicates the stability of the second critical region.

This reentrant localization feature can be seen in the energy spectrum encoded with the corresponding IPR as shown in Fig. 3(a). For clarity, we depict only the upper band of the spectrum which shows a transition from extended-critical-localized-critical-localized regions as a function of λ. A clear picture can be obtained by plotting

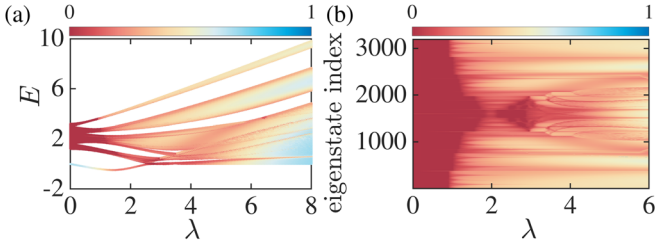

FIG. 3. (a) The upper half of the energy eigenvalue spectrum superimposed with their respective IPR shows the extended, critical, and localized states. (b) The IPR associated to the eigenstate indices as a function λ for $\delta = 2.2$ for a system of size $L = 3194$.

the IPR of the individual eigenstates as shown in Fig. 3(b). The deep red patches appearing in Figs. 3(a) and 3(b) for $2.1 < \lambda < 2.9$ indicate that some of the localized states become extended again for a range of λ. This confirms the presence of the second critical region and the second SPME. We further confirm the existence of the SPME by analyzing the IPR and the NPR for the individual eigenstates of the system in the critical regime. Figure 4(a) shows the IPR and NPR for all the eigenmodes for $\delta = 2.2$ at $\lambda = 1.2$ and 2.5 in the upper and lower panels, respectively. The plots show a clear distinction between the extended states (finite NPR) from the localized states (finite IPR) of the spectrum. A similar signature is also seen in the

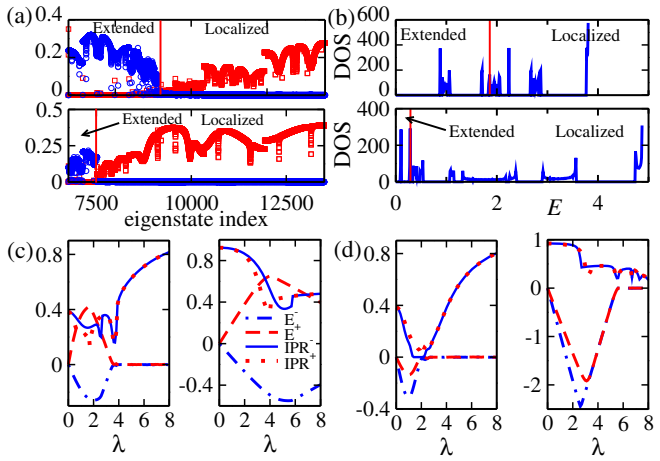

FIG. 4. (a) The IPR (red squares) and NPR (blue circles) of different eigenstates for $\delta = 2.2$ and $\lambda = 1.2$ (upper panel) and $\lambda = 2.5$ (lower panel). The states with finite IPR in the extended regime are the emerging edge modes in the fractal gaps. (b) The DOS for $\delta = 2.2$ and $\lambda = 1.2$ (upper panel) and $\lambda = 2.5$ (lower panel). The vertical lines separate the extended and localized regions. (c),(d) The edge states and the corresponding IPRs for uniform and staggered disorder, respectively, for $\delta = 1.5$ (left panel) and $\delta = 5$ (right panel). E^- (blue dot-dashed line) and E^+ (red dashed line) corresponding to the two edge states along with their IPR, i.e., IPR^- (blue solid line) and IPR^+ (red dotted line). For better visibility, the energies in the right panel of (c) are plotted as $E/4$.

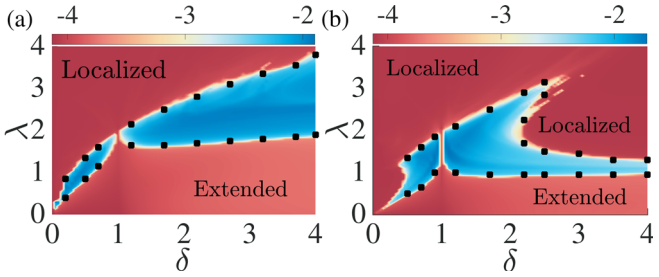

FIG. 5. The phase diagrams in δ and λ plane for (a) uniform disorder and (b) staggered disorder cases. The filled black squares are the data points obtained by examining the $\langle \mathrm{IPR} \rangle$ and $\langle \mathrm{NPR} \rangle$ plots. (See the text for details). The color code indicates the values of η.

density of states by analyzing it with the IPR of the individual states indicating the existence of the mobility edge as shown in Fig. 4(b) (see the figure caption for detail).

Phase diagram.—Finally, we present the key results in the form of a phase diagram as displayed in Fig. 5(b) for the case of staggered disorder in the δ-λ plane. The phase diagrams are obtained by computing a quantity η introduced in Ref. [26] as

$$\eta = \log_{10}[\langle \mathrm{IPR} \rangle \times \langle \mathrm{NPR} \rangle]. \tag{3}$$

The presence of the critical region (blue region bounded by the symbols) is clearly distinguished from the fully extended or the fully localized regions (red regions) in the phase diagram. Note that the critical regions are separated by a narrow passage at $\delta = 1$ (AA model), where a sharp localization transition occurs. It can be seen that for a range of δ one encounters two critical regimes with an increase in λ which is the key finding of our analysis. However, this reentrant feature does not appear in the case of uniform disorder [compare Fig. 5(a)]. We complement the above findings by directly locating the boundaries (filled squares) of the critical region by examining the values of $\langle \mathrm{IPR} \rangle$ and $\langle \mathrm{NPR} \rangle$ in the thermodynamic limit. This nontrivial feature of the reentrant localization transition and the SPME can be attributed to the competition between the hopping dimerization and the staggered disorder that renders an extended nature to some of the low-energy localized states. The detailed analysis above requires further investigation.

It is worth mentioning that the reentrant localization phenomena and the mobility edge occur in both the limits of the dimerization [see Fig. 5(b)]. Hence, an important conclusion that can be drawn at this point is that the underlying topological properties has no role in establishing the reentrant localization transition.

Edge modes.—Having analyzed the physics of the bulk spectrum, we discuss the fate of the topological zero energy edge modes as a function of the disorder strength. We note that the initially localized zero modes (at $\lambda = 0$) become energetic and finally hybridize into the bulk bands with an increase in λ for both uniform and staggered disorder cases as already shown in Figs. 1(b) (inset) and 3(a), respectively. To explicitly understand the behavior of these modes, we separately plot the edge modes as a function of λ in Fig. 4 along with their IPR. We consider two different values of δ, namely, $\delta = 1.5$ and $\delta = 5$, which represent, respectively, weak and strong dimerization limits pertaining to the topological regime. As mentioned earlier, owing to the breaking of the chiral symmetry induced by the quasiperiodic potential, both the edge modes, namely, the particle mode (E^+ shown by a dashed red line) and the hole mode (E^- shown by a dot-dashed blue line) asymmetrically separate out from each other toward the opposite bands as λ increases [Fig. 4(c)] for the case of uniform potential. However, in the case of the staggered disorder, both the edge modes move differently toward the lower band [Fig. 4(d)] [29]. Eventually, for all the cases, beyond certain critical values of λ, E^+ and E^- tend to merge with each other. We also plot the corresponding IPR for both the modes as IPR^+ (dotted red line) and IPR^- (solid blue line). It can be seen that in all four cases the IPR initially decreases and then increases as a function of λ. In the case of weak dimerization, initially the states are localized. As the value of λ increases, the states become delocalized first and then become strongly localized. On the other hand, in the case of strong dimerization, the states which are strongly localized ($\mathrm{IPR} \sim 1$) at the beginning (for small λ) remain localized forever. This analysis indicates that the behavior of the edge states as a function of λ is independent of the bulk behavior.

Conclusions.—We have studied the localization transition in a dimerized lattice with staggered quasiperiodic disorder. We show that the system undergoes a reentrant localization transition as a function of the disorder strength for a range of values of dimerization. The reentrant localization occurs in both the regimes of dimerization, and each localization transition is associated with the SPME. We confirm this finding by examining the participation ratios, the single-particle spectrum, and the behavior of the individual eigenstates and present a phase diagram depicting all the above findings. For completeness, we also analyze the phase diagram in the case of uniform disorder which shows the usual localization transition and the SPME. In the end, we discuss the fate of the zero energy edge modes as a function of disorder strength which were initially localized in the absence of any disorder due to the topological nature of the model.

The reentrant feature may reveal interesting physics in transport and dynamical properties of quantum particles. An immediate extension could be to study the stability of this reentrant phenomenon in the context of many-body localization. Because of the phenomenal experimental progress in systems of ultracold atoms in optical lattices

to simulate dimerized latticed [30,31], quasiperiodic systems [21,23] and the recent experiment on a disorder-induced topological phase transition using ^{171}Yb [32], our findings can, in principle, be simulated in the state-of-the-art quantum gas experiments.

We thank Luis Santos and Subroto Mukerjee for useful discussions. S. B. acknowledges funding from Science and Engineering Research Board (SERB), India (Project No. EMR/2015/001039). B. T. acknowledges support from Turkish Academy of Sciences (TUBA) Project No. AD-21 and the Scientific and Technological Research Council of Turkey (TUBITAK). T. M. acknowledges financial support from Science and Engineering Research Board (SERB), India (Project No. ECR/2017/001069).

Note added.—Recently, we became aware of an interesting recent work related to localization transition in an interpolating Aubry-André-Fibonacci model [33]. The model is shown to exhibit a cascade of band selective localization and delocalization transitions while transiting from the AA into a Fibonacci model.

[1] P. A. Lee and T. V. Ramakrishnan, Rev. Mod. Phys. **57**, 287 (1985).
[2] P. W. Anderson, Phys. Rev. **109**, 1492 (1958).
[3] T. Schwartz, G. Bartal, S. Fishman, and M. Segev, Nature (London) **446**, 52 (2007).
[4] H. Hu, A. Strybulevych, J. Page, S. E. Skipetrov, and B. A. van Tiggelen, Nat. Phys. **4**, 945 (2008).
[5] K. Drese and M. Holthaus, Phys. Rev. Lett. **78**, 2932 (1997).
[6] G. Semeghini, M. Landini, P. Castilho, S. Roy, G. Spagnolli, A. Trenkwalder, M. Fattori, M. Inguscio, and G. Modugno, Nat. Phys. **11**, 554 (2015).
[7] F. Jendrzejewski, A. Bernard, K. Mueller, P. Cheinet, V. Josse, M. Piraud, L. Pezzé, L. Sanchez-Palencia, A. Aspect, and P. Bouyer, Nat. Phys. **8**, 398 (2012).
[8] W. R. McGehee, S. S. Kondov, W. Xu, J. J. Zirbel, and B. DeMarco, Phys. Rev. Lett. **111**, 145303 (2013).
[9] G. Roati, C. D'Errico, L. Fallani, M. Fattori, C. Fort, M. Zaccanti, G. Modugno, M. Modugno, and M. Inguscio, Nature (London) **453**, 895 (2008).
[10] J. Billy, V. Josse, Z. Zuo, A. Bernard, B. Hambrecht, P. Lugan, D. Clément, L. Sanchez-Palencia, P. Bouyer, and A. Aspect, Nature (London) **453**, 891 (2008).
[11] S. Aubry and G. André, Ann. Israel Phys. Soc. **3**, 18 (1980).
[12] S. Das Sarma, A. Kobayashi, and R. E. Prange, Phys. Rev. Lett. **56**, 1280 (1986).
[13] J. Biddle and S. Das Sarma, Phys. Rev. Lett. **104**, 070601 (2010).
[14] S. Ganeshan, J. H. Pixley, and S. Das Sarma, Phys. Rev. Lett. **114**, 146601 (2015).
[15] M. L. Sun, G. Wang, N. B. Li, and T. Nakayama, Europhys. Lett. **110**, 57003 (2015).
[16] S. Gopalakrishnan, Phys. Rev. B **96**, 054202 (2017).
[17] A. Purkayastha, A. Dhar, and M. Kulkarni, Phys. Rev. B **96**, 180204(R) (2017).
[18] N. Mott, J. Phys. C **20**, 3075 (1987).
[19] D. J. Boers, B. Goedeke, D. Hinrichs, and M. Holthaus, Phys. Rev. A **75**, 063404 (2007).
[20] X. Li, X. Li, and S. Das Sarma, Phys. Rev. B **96**, 085119 (2017).
[21] H. P. Lüschen, S. Scherg, T. Kohlert, M. Schreiber, P. Bordia, X. Li, S. Das Sarma, and I. Bloch, Phys. Rev. Lett. **120**, 160404 (2018).
[22] F. A. An, E. J. Meier, and B. Gadway, Phys. Rev. X **8**, 031045 (2018).
[23] F. A. An, K. Padavić, E. J. Meier, S. Hegde, S. Ganeshan, J. H. Pixley, S. Vishveshwara, and B. Gadway, Phys. Rev. Lett. **126**, 040603 (2021).
[24] W. P. Su, J. R. Schrieffer, and A. J. Heeger, Phys. Rev. Lett. **42**, 1698 (1979).
[25] S. Y. Jitomirskaya, Ann. Math. **150**, 1159 (1999).
[26] X. Li and S. Das Sarma, Phys. Rev. B **101**, 064203 (2020).
[27] J. Sokoloff, Phys. Rep. **126**, 189 (1985).
[28] See Supplemental Material at http://link.aps.org/supplemental/10.1103/PhysRevLett.126.106803 for the finite size scaling of the participation ratios.
[29] With a configuration where λ has a positive sign at the leftmost site and a negative sign at the rightmost site of the chain.
[30] M. Lohse, C. Schweizer, O. Zilberberg, M. Aidelsburger, and I. Bloch, Nat. Phys. **12**, 350 (2016).
[31] S. de Léséleuc, V. Lienhard, P. Scholl, D. Barredo, S. Weber, N. Lang, H. P. Büchler, T. Lahaye, and A. Browaeys, Science **365**, 775 (2019).
[32] S. Nakajima, N. Takei, K. Sakuma, Y. Kuno, P. Marra, and Y. Takahashi, arXiv:2007.06817.
[33] V. Goblot, A. Štrkalj, N. Pernet, J. L. Lado, C. Dorow, A. Lemaître, L. Le Gratiet, A. Harouri, I. Sagnes, S. Ravets, A. Amo, J. Bloch, and O. Zilberberg, Nat. Phys. **16**, 832 (2020).